PERFECT RECONSTRUCTION AM-FM IMAGE MODELS

Roy A. Sivley and Joseph P. Havlicek

School of Electrical and Computer Engineering
University of Oklahoma, Norman, OK 73019 USA

ABSTRACT

For the first time, we present an AM-FM image model that, in addition to being remarkably consistent with human visual perception, also provides perfect reconstruction of the image and is thus suitable for synthesis as well as analysis applications. We employ a non-separable coiflet-based wavelet filterbank with channels that are both orientation selective and jointly localized. The analysis responses define the AM-FM image components, which we demodulate analytically using a new, high-quality 2-D phase unwrapping algorithm coupled with a spline-based phase model. The amplitude and frequency modulations obtained with this approach correspond remarkably well with human visual perception of the salient image structures, suggesting that this invertible model could form the basis for a general theory of image processing in the modulation domain.

Index Terms— Amplitude modulation, frequency modulation, image reconstruction

1. INTRODUCTION

AM-FM models characterize nonstationary image structure using amplitude and frequency modulations that generalize the Fourier representation. These models have proven utility in computer vision and image analysis applications, including texture segmentation and classification, 3-D shape from texture, texture-based stereopsis, fingerprint classification, CBIR, and repair of damaged textures [1]. For a complex-valued image $t : \mathbb{R}^2 \rightarrow \mathbb{C}$, which may be associated with a real-valued image using the multidimensional Hilbert transform [2], the K-component AM-FM model is given by

$$t(\mathbf{x}) = \sum_{m=1}^{K} y_m(\mathbf{x}) = \sum_{m=1}^{K} a_m(\mathbf{x}) \exp[j\varphi_m(\mathbf{x})], \qquad (1)$$

where each $y_m(\mathbf{x})$ is an AM-FM component with amplitude modulation $a_m(\mathbf{x})$ and frequency modulation $\nabla\varphi_m(\mathbf{x})$. These modulation functions define the *modulation domain image representation*, which has been previously estimated using the continuous and discrete demodulation algorithms of [3, 4].

Existing demodulation algorithms are strongly dependent upon the use of jointly localized analysis filters and on the approximation of the AM and FM functions from the filter responses. These approximations are accurate when applied to AM-FM components $y_m(\mathbf{x})$ that are *locally coherent* in the sense that the AM and FM functions satisfy certain local smoothness constraints given in [4–6]; however, there can be large scale approximation errors in image regions that do not admit sufficiently smoothly varying modulations. Thus, demodulation accuracy depends upon the ability of the filterbank to deliver a decomposition (1) wherein the components are locally coherent. Such filterbanks were studied in [4, 7], where it was shown that the filters must possess a high degree of localization in both space and frequency, which strongly suggests the use of Gabor filters.

We seek a modulation domain image representation that can both provide perfect reconstruction and be used to synthesize *new* images obtained by performing image processing operations in the modulation domain. This cannot be provided by existing AM-FM computational paradigms because of inherent approximations in the demodulation algorithms and because the Gabor filters that are typically used fail to yield an orthogonal image decomposition. Two systems are needed to develop a perfect reconstruction AM-FM image model: a jointly localized perfect reconstruction filterbank which yields AM-FM components that agree with human visual perception and a demodulation algorithm that provides amplitude, phase, and frequency estimates that are *consistent* with both the nonstationary image structure and the known pixel values. Orthogonal wavelet decompositions are attractive choices for designing perfect reconstruction filterbanks, and it is natural to choose a continuous phase model $\varphi_m(\mathbf{x})$ to allow the analytic definition of the frequency modulation $\nabla\varphi_m(\mathbf{x})$; however, a direct implementation of either of these concepts yields AM and FM functions that do not necessarily agree with image structure because of the multiple resolutions of the wavelet coefficients and because of the well-known multidimensional phase wrapping problem.

In this paper, we present a new perfect reconstruction AM-FM image model which delivers modulation functions consistent with human visual perception. We isolate AM-FM components using a 2-D wavelet filterbank based on the six-point coiflet, which we further decompose into highly localized, orientation selective sub-channels. This filterbank is implemented in a maximally decimated parallel structure that exhibits excellent joint localization [8] and retains the image resolution in each AM-FM component. A new, high-quality 2-D phase unwrapping algorithm is applied to each component to obtain phase modulations $\varphi_m(\mathbf{x})$ that are consistent with FM functions $\nabla\varphi_m(\mathbf{x})$ lying in the space of tensor product cubic splines.

2. PERFECT RECONSTRUCTION FILTERBANK

To decompose an image into AM-FM components with visually significant structure, we employ a 2-D wavelet filterbank based on the six-point coiflet. The design is a modified version of the filterbank described in [9], which employed the six-point Daubechies wavelet. For each dimension, a 4-level discrete wavelet transform is defined with an additional low- and high-pass decomposition applied to each high-pass output. This ensures that the resulting separable 2-D filters are defined on symmetric dyadic partitions that densely sample the frequency plane. The Noble identities are used to construct

This work was supported in part by the U.S. Army Research Laboratory and the U.S. Army Research Office under grant W911NF-04-1-0221.

the equivalent, maximally decimated parallel structure consisting of a bank of analysis filters, intermediate down-samplers and up-samplers, and a bank of synthesis filters. This structure is attractive for AM-FM image modeling because it exhibits excellent joint localization properties [8] which generally correspond to locally coherent AM-FM image components [4, 7].

A side-effect of the Noble identities is the up-sampling of the analysis and synthesis filter impulse responses, which can create significant side lobes in their frequency responses. This characteristic can be seen in the log-magnitude frequency response of the filterbank channel depicted in Fig. 1(a). Additionally, non-separable filters are required to obtain individual texture orientations in the AM-FM components. To address these issues, we take advantage of the loci of zeros that occur in the frequency responses to further decompose each channel into a sum of non-separable, highly localized subchannels. Fig. 1(b) depicts the log-magnitude frequency response of one such sub-channel extracted from the separable channel shown in Fig. 1(a).

Since it is of interest to obtain AM-FM components that embody the visually significant nonstationary structure present in the image, we *define* the AM-FM components $y_m(\mathbf{x})$ to be the full-resolution outputs of the *analysis* filters. The image can then be perfectly reconstructed by applying the associated down-samplers, up-samplers, and synthesis filters to the components $y_m(\mathbf{x})$ and summing the results. Although this framework does not yield the decomposition described by (1), such a decomposition is not unique, and thus, the AM-FM components obtained here will be both valid and representative of visually significant image structure.

3. CONSISTENT DEMODULATION

Given the AM-FM image components $y_m(\mathbf{x})$, we want to compute the AM functions $a_m(\mathbf{x})$ and FM functions $\nabla\varphi_m(\mathbf{x})$. In continuous space, these may be obtained by [4]

$$a_m(\mathbf{x}) = |y_m(\mathbf{x})|, \tag{2}$$

$$\nabla\varphi_m(\mathbf{x}) = \mathrm{Re}\left[\frac{\nabla y_m(\mathbf{x})}{j y_m(\mathbf{x})}\right]. \tag{3}$$

Although (2) may also be applied directly to discrete images, (3) cannot due to the gradient operator which is well-defined only in continuous space. This deficiency may be circumvented by fitting the samples $y_m(\mathbf{k})$ with continuous space interpolants for which the derivative is well-defined, as was done in [10]. However, in this case, the phase samples $\varphi_m(\mathbf{k})$ are only available as *principal values* in the range $(-\pi, \pi]$, which exhibit substantial and undesirable phase discontinuities at the branch cuts, leading to FM functions which correspond to these branch cuts but not to any visually meaningful structure in the image.

Multidimensional phase unwrapping has been studied extensively in a general sense and in the context of SAR interferometry, magnetic resonance imaging, and network flow analysis [11–16]. However, nearly all existing phase unwrapping algorithms rely on the assumption that the inter-pixel differences in the unwrapped phase $\varphi_m(\mathbf{k})$ are bounded by π radians, and the violation of this constraint, which is common for practical images, is referred to as *phase aliasing*. Although many methods have been proposed to identify and accommodate image regions that exhibit phase aliasing [11–14] or to simply calculate the phase function that minimizes a particular functional norm [15, 16], our objective is to calculate an unwrapped phase which admits a gradient field that is consistent with human visual perception of the image.

We begin by seeking an unwrapped phase that is in agreement with continuous phase gradient estimates obtained from the unit-amplitude model

$$\rho_m(\mathbf{x}) = \exp[j\overline{\varphi_m}(\mathbf{x})], \tag{4}$$

where $\overline{\varphi_m}(\mathbf{x})$ is the phase modulation $\varphi_m(\mathbf{x})$ that has been interpolated at ambiguous points where $a_m(\mathbf{x}) \approx 0$. Using the tensor product cubic spline framework of Unser *et al.* [17] and letting ∂^2 denote the second derivative operator, the second phase derivative vector is estimated by

$$\begin{aligned}\partial^2\varphi_m(\mathbf{x}) &\approx \partial^2\widehat{\varphi_m}(\mathbf{x}) \\ &= \mathrm{Re}\left[\frac{\partial^2\rho_m(\mathbf{x})}{j\rho_m(\mathbf{x})}\right] + \mathrm{Im}\left[\left(\frac{\nabla\rho_m(\mathbf{x})}{j\rho_m(\mathbf{x})}\right)^2\right],\end{aligned} \tag{5}$$

which is rigorous for *any* C^2 phase interpolant. By minimizing the error

$$\varepsilon = \sum_{\mathbf{k}} \left|\partial^2\psi_m(\mathbf{k}) - \partial^2\widehat{\varphi_m}(\mathbf{k})\right|^2, \tag{6}$$

we compute the unwrapped phase $\psi_m(\mathbf{k})$ with second derivatives that are closest to the estimates $\partial^2\widehat{\varphi_m}(\mathbf{k})$ in the least-squares sense. Least-squares phase unwrapping has been previously studied using the assumption that the phase differences are less than π radians [11–14] and using the gradient of a cubic spline phase model [18]. The second cubic spline derivative is used here to reduce the degrees of freedom in the solution of [18] to an additive constant. The 1-D filter $h(k)$ used to compute the cubic spline second derivative is defined by the z-transform [17]

$$H(z) = \frac{6z - 12 + 6z^{-1}}{z + 4 + z^{-1}}, \tag{7}$$

which can be used to express the error in (6) as

$$\varepsilon = \sum_{i=1}^{2}\sum_{\mathbf{k}}\left(\psi_m(\mathbf{k}) * h(\mathbf{e}_i^T\mathbf{k}) - \mathbf{e}_i^T\partial^2\widehat{\varphi_m}(\mathbf{k})\right)^2, \tag{8}$$

where $\mathbf{e}_i$ is the unit vector in the k_i direction.

The least-squares phase solution $\psi_m(\mathbf{k})$ will agree with the estimated phase derivatives and, hence, represents the visually significant structure of the AM-FM image component; however, it will not generally be consistent with the known principal phase values of the original component obtained from the analysis filterbank because the derivative estimates in (5) fail to lie in the spline space used to model the signals (4). This problem is overcome by embedding the principal phase values in a scaled phase function $\gamma\psi_m(\mathbf{k})$ for some large $\gamma \in \mathbb{R}$. Thus, we *define* the phase modulation by

$$\varphi_m(\mathbf{k}) = W\{\overline{\varphi_m}(\mathbf{k})\} + 2\pi b_m(\mathbf{k}) \approx \gamma\psi_m(\mathbf{k}), \tag{9}$$

where $W\{\overline{\varphi_m}(\mathbf{k})\}$ is the known wrapped phase and the branch function $b_m(\mathbf{k})$ is defined as

$$b_m(\mathbf{k}) = \mathrm{round}\left(\frac{\gamma\psi_m(\mathbf{k}) - W\{\overline{\varphi_m}(\mathbf{k})\}}{2\pi}\right). \tag{10}$$

Taking the cubic spline gradient of (9), we obtain the FM function $\nabla\varphi_m(\mathbf{x})$, which can be made arbitrarily close to the desired least-squares phase gradient by the choice of γ:

$$\left|\frac{1}{\gamma}\varphi_m(\mathbf{x}) - \psi_m(\mathbf{x})\right| \le \frac{\pi}{|\gamma|}. \tag{11}$$

In practice, we choose $\gamma = 300$, which ensures that the bound is generally less than 1%. However, *independent* of this value, the consistent phase modulation $\varphi_m(\mathbf{k})$ can be recovered by integrating the spline gradient $\nabla\varphi_m(\mathbf{x})$, thereby enabling perfect reconstruction of the image component $y_m(\mathbf{k}) = a_m(\mathbf{k})\exp[j\varphi_m(\mathbf{k})]$.

4. EXPERIMENTAL RESULTS

The filterbank and demodulation algorithm described in Sections 2 and 3 were applied to the *Lena* image depicted in Fig. 1(c). The log-magnitude frequency response of one of the separable filterbank channels is shown in Fig. 1(a), and the log-magnitude frequency response of one of its non-separable, orientation selective sub-channels is shown in Fig. 1(b). The AM-FM component obtained from this sub-channel is shown in Fig. 1(d), where the nonstationary structure of the hat brim, the mirror frame, and the subject's reflection in the mirror are evident. Fig. 1(e) and Fig. 1(f) show the computed AM and FM functions for this component, where Fig. 1(e) depicts the FM vectors overlaying the AM intensity. The FM vectors shown in Fig. 1(f) are scaled by the AM function to accentuate the smooth variations of the modulation functions across the image structure captured by this component. The AM and FM functions and the component itself all exhibit visually significant structure from the original image. Moreover, these quantities agree with human visual perception as evidenced by the increased AM in the regions of high contrast surrounding the hat brim and the mirror frame and by the orientation of the FM vectors around these structures.

5. CONCLUSION

We have presented a new perfect reconstruction AM-FM image model that provides amplitude and frequency modulations that are consistent with human visual perception. This model provides the first modulation domain image representation that can be used for a wide variety of image analysis and computer vision applications as well as to *exactly* reconstruct the original image from the model. Thus, this representation provides a long-awaited framework for the formulation of a general theory of image processing in the modulation domain.

6. REFERENCES

[1] J. P. Havlicek, P. C. Tay, and A. C. Bovik, "AM-FM image models: Fundamental techniques and emerging trends," in *Handbook of Image and Video Processing*, A. C. Bovik, Ed., pp. 377–395. Elsevier Academic Press, Burlington, MA, 2 edition, 2005.

[2] J. P. Havlicek, J. W. Havlicek, and A. C. Bovik, "The analytic image," in *Proc. IEEE Int'l. Conf. Image Proc.*, Santa Barbara, CA, Oct. 26-29, 1997.

[3] P. Maragos and A. C. Bovik, "Image demodulation using multidimensional energy separation," *J. Opt. Soc. Amer. A*, vol. 12, no. 9, pp. 1867–1876, Sep. 1995.

[4] J. P. Havlicek, D. S. Harding, and A. C. Bovik, "Multidimensional quasi-eigenfunction approximations and multicomponent AM-FM models," *IEEE Trans. Image Proc.*, vol. 9, no. 2, pp. 227–242, Feb. 2000.

[5] P. Maragos, J. F. Kaiser, and T. F. Quatieri, "On amplitude and frequency demodulation using energy operators," *IEEE Trans. Signal Proc.*, vol. 41, no. 4, pp. 1532–1550, Apr. 1993.

[6] P. Maragos, J. F. Kaiser, and T. F. Quatieri, "Energy separation in signal modulations with applications to speech analysis," *IEEE Trans. Signal Proc.*, vol. 41, no. 10, pp. 3024–3051, Oct. 1993.

[7] A. C. Bovik, N. Gopal, T. Emmoth, and A. Restrepo, "Localized measurement of emergent image frequencies by Gabor wavelets," *IEEE Trans. Info. Theory*, vol. 38, no. 2, pp. 691–712, Mar. 1992.

[8] P. C. Tay and J. P. Havlicek, "Joint uncertainty measures for maximally decimated M-channel prime factor cascaded wavelet filter banks," in *Proc. IEEE Int'l. Conf. Image Proc.*, Barcelona, Spain, Sep. 14-17 2003, vol. I, pp. 1033–1036.

[9] P. C. Tay and J. P. Havlicek, "Frequency implementation of discrete wavelet transforms," in *Proc. IEEE Southwest Symp. Image Anal., Interp.*, Lake Tahoe, NV, Mar. 28-30 2004, pp. 167–171.

[10] D. Dimitriadis and P. Maragos, "An improved energy demodulation algorithm using splines," in *Proc. IEEE Int'l. Conf. Acoust., Speech, Signal Proc.*, Salt Lake City, UT, May 7-11, 2001, pp. 3481–3484.

[11] H. Takajo and T. Takahashi, "Noniterative method for obtaining the exact solution for the normal equation in the least-squares phase estimation from the phase difference," *J. Opt. Soc. Am. A*, vol. 5, no. 11, pp. 1818–1827, Nov. 1988.

[12] D. C. Ghiglia and L. A. Romero, "Robust two-dimensional weighted and unweighted phase unwrapping that uses fast transforms and iterative methods," *J. Opt. Soc. Am. A*, vol. 11, no. 1, pp. 107–117, Jan. 1994.

[13] U. Spagnolini, "2-D phase unwrapping and phase aliasing," *Geophys.*, vol. 58, no. 9, pp. 1324–1334, Sep. 1993.

[14] S. M. -H. Song, S. Napel, N. J. Pelc, and G. H. Glover, "Phase unwrapping of MR phase images using Poisson equation," *IEEE Trans. Image Proc.*, vol. 4, no. 5, pp. 667–676, May 1995.

[15] T. J. Flynn, "Two-dimensional phase unwrapping with minimum weighted discontinuity," *J. Opt. Soc. Am. A*, vol. 14, no. 10, pp. 2692–2701, Oct. 1997.

[16] C. W. Chen and H. A. Zebker, "Network approaches to two-dimensional phase unwrapping: Intractability and two new algorithms," *J. Opt. Soc. Am. A*, vol. 17, no. 3, pp. 401–414, Mar. 2000.

[17] M. Unser, A. Aldroubi, and M. Eden, "B-spline signal processing: Part II–efficient design and applications," *IEEE Trans. Signal Proc.*, vol. 41, no. 2, pp. 834–848, Feb. 1993.

[18] R. A. Sivley and J. P. Havlicek, "Multidimensional phase unwrapping for consistent APF estimation," in *Proc. IEEE Int'l. Conf. Image Proc.*, Genoa, Italy, Sep. 11-14, 2005, vol. II, pp. 458–461.

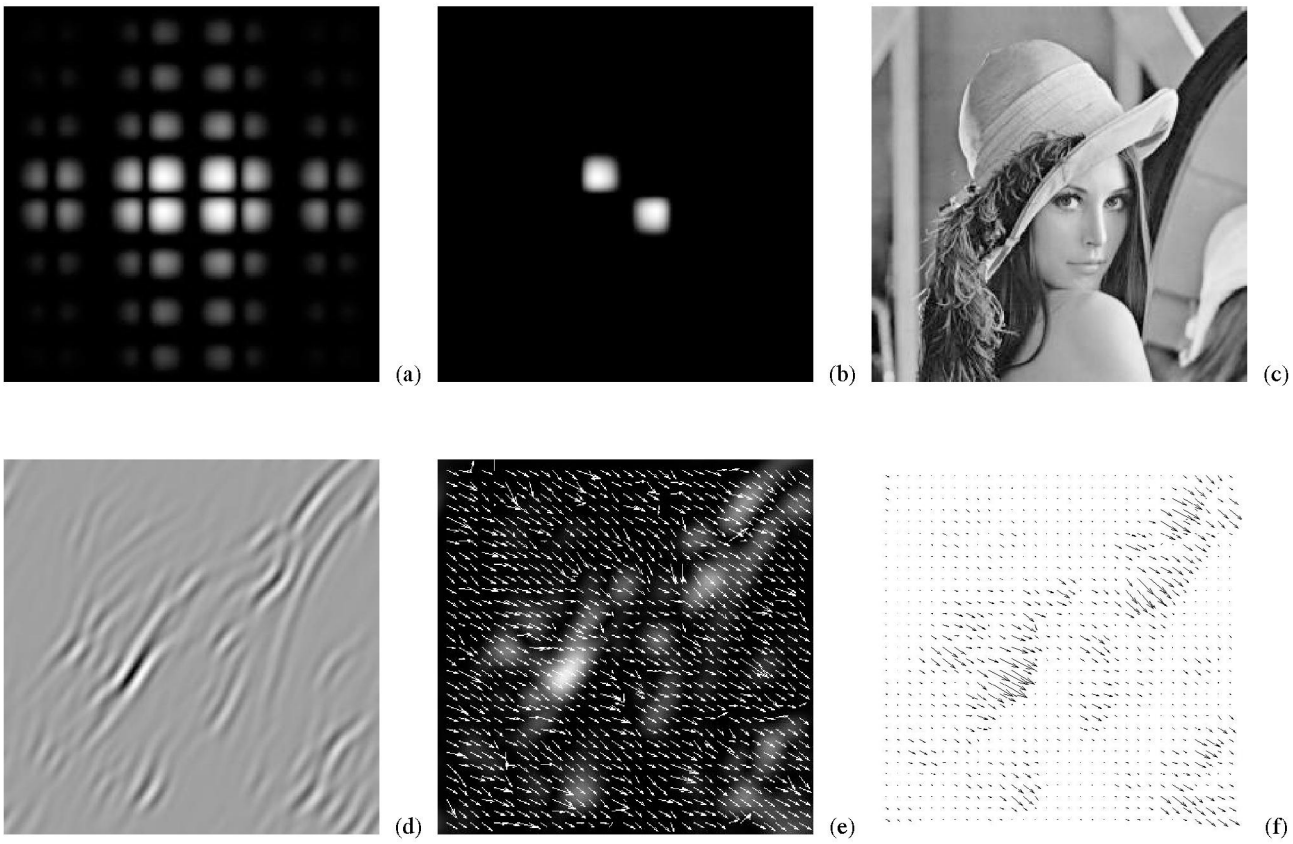

Fig. 1. Example. (a) Frequency response of one of the separable wavelet filterbank channels. (b) One of the non-separable, orientation selective sub-channels obtained from (a). (c) Original *Lena* image. (d) AM-FM image component obtained from filtering image (c) with channel (b). (e) AM and FM functions computed from (d). (f) FM function scaled by the AM function.